We are IntechOpen, the world's leading publisher of Open Access books Built by scientists, for scientists

4,800
Open access books available

122,000
International authors and editors

135M
Downloads

Our authors are among the

154
Countries delivered to

TOP 1%
most cited scientists

12.2%
Contributors from top 500 universities

CLARIVATE ANALYTICS BOOK CITATION INDEX INDEXED

WEB OF SCIENCE™

Selection of our books indexed in the Book Citation Index in Web of Science™ Core Collection (BKCI)

Interested in publishing with us?
Contact book.department@intechopen.com

Numbers displayed above are based on latest data collected.
For more information visit www.intechopen.com

5

Non-Destructive Testing Techniques for Detecting Imperfections in Friction Stir Welds of Aluminium Alloys

Pedro Vilaça[1,2] and Telmo G. Santos[3]
[1]*IDMEC, Instituto de Engenharia Mecânica, Av. Rovisco Pais, 1, 1049-001 Lisboa*
[2]*IST-UTL, Instituto Superior Técnico, Av. Rovisco Pais, 1049-001 Lisboa*
[3]*UNIDEMI, DEMI, Faculdade de Ciências e Tecnologia, UNL, 2829-516 Caparica*
Portugal

1. Introduction

The invention of Friction Stir Welding (FSW) (Thomas, 2009) has contributed for a significant push forward in the weldability criteria for many engineering materials and the concept of how they can be mechanically processed in solid state. From the many materials processed by FSW the most remarkable results were obtained for the aluminium and all its alloys including wrought and cast original conditions. The main technological procedures and parameters are presented and most relevant tool features and architecture are established (Vilaça, 2003). Some industrial applications of FSWelds of aluminium alloys are also summarized.

The quality of FSWelds of aluminium and its alloys is easy to reproduce and usually excellent, exceeding for some particular conditions the performance of base materials. Nevertheless, some imperfections can occur. The geometry, location, and microstructural nature of these imperfections will be established and classified for butt and overlap joints, which are the basic geometries enabling the production of all the remaining joint configurations, by combination of the previous. These imperfections bear no resemblance to the imperfections typically found in aluminium fusion welds. Consequently, it is difficult or even impossible, to identify all the FSWelds imperfections with commercially available conventional and advanced non-destructive testing (NDT) techniques. A paradigmatic example is the micro defects located at the root of conventional FSWeld joints with less than 100-50 μm. This state-of-the-art has been revealed as one important drawback preventing a wider transition of FSW to industrial applications, mainly focusing those where the quality standards are highly demanding and pursue the total quality assurance paradigm.

The review of physical fundaments and some technological features of the different NDT concepts is included supporting the presentation of the following content of the present chapter (Santos, 2009).

The assessment of the applicability of the conventional and advanced available NDT techniques to the most relevant FSW imperfections is established. The lack of assertiveness of the available NDT techniques in detecting the FSW joint imperfections are identified emphasizing the importance of the most recent new advances in the NDT technological

field, regarding the support of the industrial production of FSWelds involving aluminium and aluminium alloys.
To solve this lack of technological capacity in detecting non-destructively some imperfections in FSWelds, which may significantly affect the performance of the weld joints, many research and technological development projects are being undertaken and some of the most relevant results are presented in this chapter. The presentation of these new developments starts with the presentation of a system with acronym: QNDT_FSW, which consist of an integrated, on-line, NDT inspection system for FS welds, which employs a data fusion algorithm with fuzzy logic and fuzzy inference functions. It works by analyzing complementary and redundant data acquired from several NDT techniques (ultrasonic, Time of Flight Diffraction (ToFD), and eddy currents) to generate a synergistic effect that is used by the software to improve the confidence of detecting imperfections.
The next NDT development presented is a innovative system consisting of a new patented eddy current (EC) probes; electronic generation, conditioning and signal acquisition; automated mechanized scanning and dedicated NDT software. The new EC probe allows a 3D induced current in the material, and an easy interpretation of the signal based, not on the absolute value, but on a comprehensible perturbation of the signal. The results from an analytical simulation fully agree with the experiments.The experimental results clearly show that this system is able to detect imperfections around 50 μm, which contribute to increase the reliability on NDT of micro imperfections.

2. FSW process fundaments

2.1 General features

Friction stir welding (FSW) is a process for joining workpieces in the solid-phase, using an intermediate non-consumable tool, with a somewhat complex shoulder and probe profile, made of material that is harder than the workpiece material being welded. FSW can be regarded as an autogenous keyhole joining technique without the creation of liquid metal (Thomas et al., 1991).
The rotating tool, is plunged into the weld joint and forced to traverse along the joint line, heating the abutting components by interfacial and internal friction, thus producing a weld joint by extruding, forging and stirring the materials from the workpieces in the vicinity of the tool. The basic principles of the process and some nomenclature are represented in Figure 1.
This machine tool based process is recurrently considered the most important recent development in the welding technology, saving costs and weight for a steadily expanding range of applications of Lightweight Metallic Structures. As evidence of the disruptive character of the FSW process, world-wide research and development centers have chosen this issue has as a primary priority and the many significant advantages of FSW have rapidly been transferred to industry. Initially to the most demanding quality standards industrial applications and more recently spread to a wide range of structural and non-structural components.

2.2 Parameters

One important advantage of FSW is the Total Quality Assurance of results once all the process parameters are correctly established and monitored during the processing. The process parameters are easy to assess because FSW is mostly a mechanical welding process

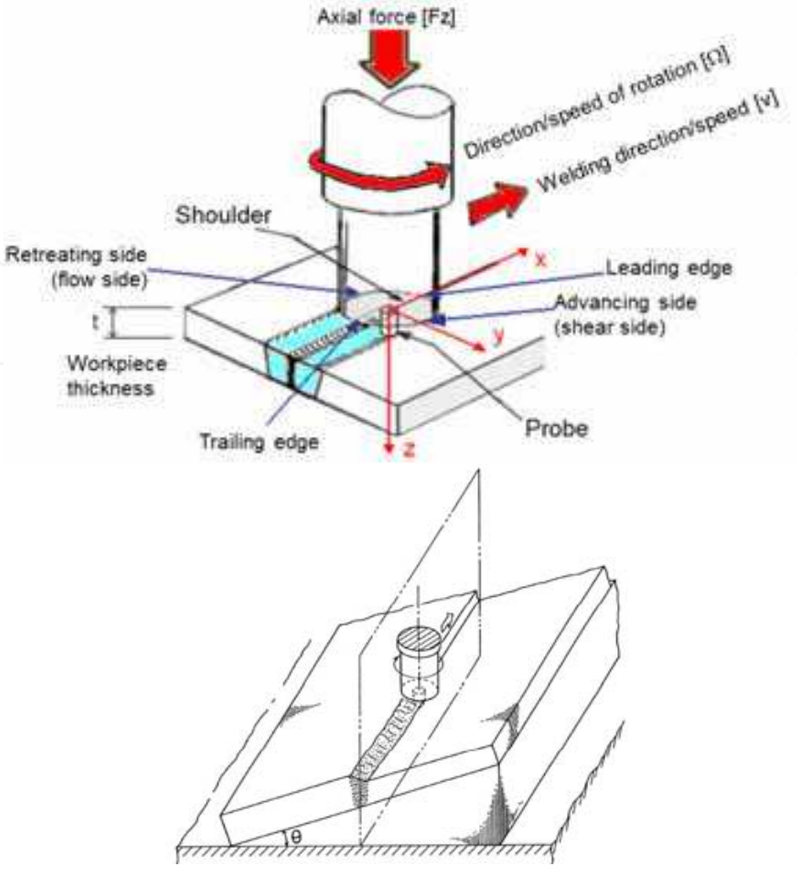

Fig. 1. Representation of some of the main parameters and nomenclature of FSW joints

where the results do not depend on difficult to control conditions, such as, environmental conditions or operator skills.

For achieving the Total Quality Assurance conditions, one important requirement is a strong, stiff machine and clamping system, able to react and apply the necessary load onto the workpiece via the tool, allowing to create and maintain the correct conditions.

In order to optimize the performance of the resultant FSW joint, and considering that the FSW results can be sensitive to variations of some welding parameters, it is important to identify and understand possible interactions between the welding parameters. The main FSW process parameters are the following:

1. FSW tool geometry;
2. Travel speed, v [mm/min];
3. Rotation speed, Ω [rpm];
4. Rotation direction [CW or CCW];
5. Tool rotational axis eccentricity [mm];
6. Vertical downward forging force, F_z [N];
7. Plunge distance of probe bottom to anvil [mm];
8. Plunge speed, [mm/s];
9. Dwell time, [s];
10. Tilt angle, α [º];
11. Concordance angle, θ [º];

12. Start position, (x,y) [mm];
13. End position, (x,y) [mm];
14. FSW control mode during weld [Force/Position];
15. Initial temperature/interpass temperature of welded components.

2.3 FSW tools

The shoulder and probe geometry are the most important feature that influences the final properties of the weld seam.

- Shoulder: outer diameter + shape + features;
- Probe: length +diameter along the length + shape + features;
- Oblique angle between probe axis and tool rotation axis;
- Ratio between static volume and dynamic volume of the probe;
- Tool axis eccentricity relatively to real tool rotation axis.

The most common FSW tools used in industrial applications are the mono-bloc conventional ones, composed by a threaded probe and a shoulder (Figure 2). These tools are limited to single thickness plates, since the probe length cannot be changed.

In laboratorial conditions this tool configurations becomes inadequate, since it is necessary to investigate the influence of different tool geometries (probe and shoulder), or it is necessary welding several plates with different thicknesses. Modular and adjustable tools are needed to meet these requirements. In Figure 3 it is shown a modular FSW tool designed for allowing the adjustment of the probe length by a vertical regulation of a screw. This FSW tool concept also allows the change and combination of different probe and shoulder geometries due to their symmetry (Figure 3 c).

Figure 4 show an alternative design consisting of a modular dual FSW tool with forced cooling.

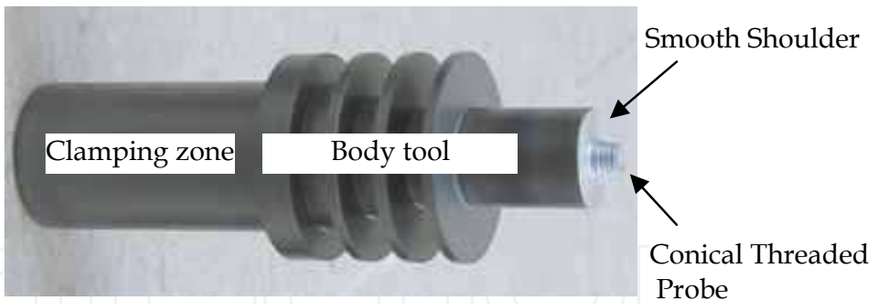

Fig. 2. Conventional FSW mono-bloc tool

A proposed design criterion for producing scrolled shoulders is established in (1) and (2) in polar coordinates. Figure 5, represents the scrolls for different Scroll Pitchs.

$$ScrollPitch \propto \frac{NScr \times v}{\Omega} \tag{1}$$

$$\text{Scroll Position} = \begin{cases} R = R_{shoulder} - \dfrac{ScrollPitch \times \beta \times (R_{shoulder} - R_{\text{int}})}{2\pi} \\ \beta = \left[0.. \dfrac{2\pi}{ScrollPitch} \right] \end{cases} \tag{2}$$

Where:

NScr – Number (integer) of scrolls (this value is set to a maximum of *NScr=4)*;

$R_{shoulder}$ – Exterior radius of the shoulder [mm];

R_{int} – Interior radius of the shoulder [mm];

β – Angle starting with the scroll on the exterior diameter of the shoulder and ending where the scroll ends at the interior radius of the shoulder [rad].

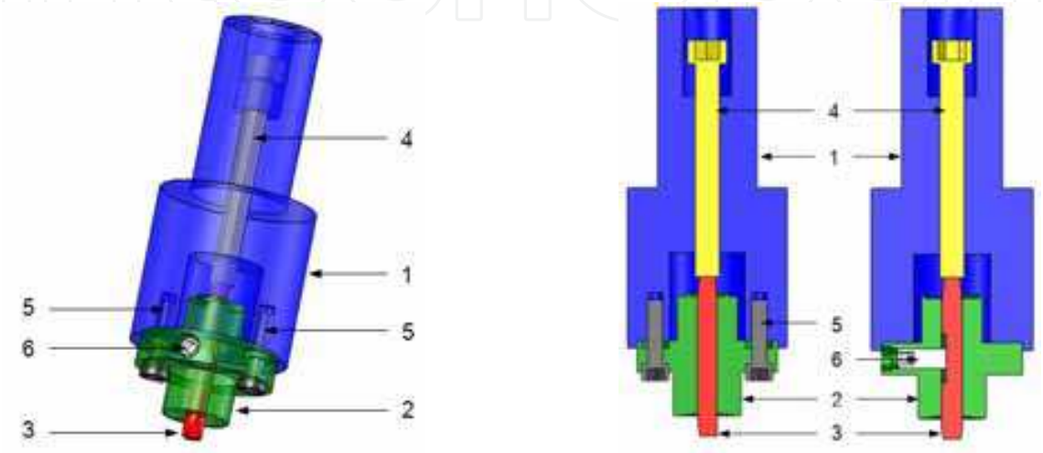

(a) (b)

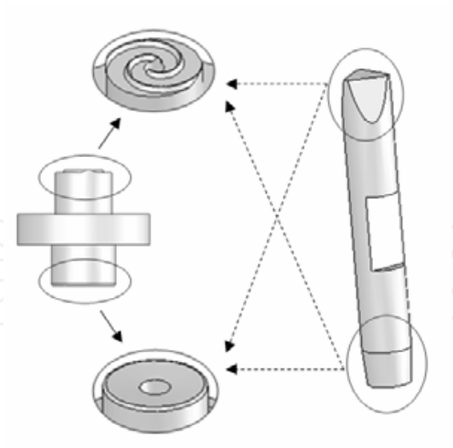

(c)

Fig. 3. Modular dual FSW tool. a) 3D view of assembly, b) Cutaway view in two perpendicular planes, c) Detail of geometric duality of the dual basis and probe dual. Nomenclature: main body (1), dual shoulder (2), dual-probe (3), vertical adjustment screw (4), bolts of the dual basis (5), dual screw probe (6).

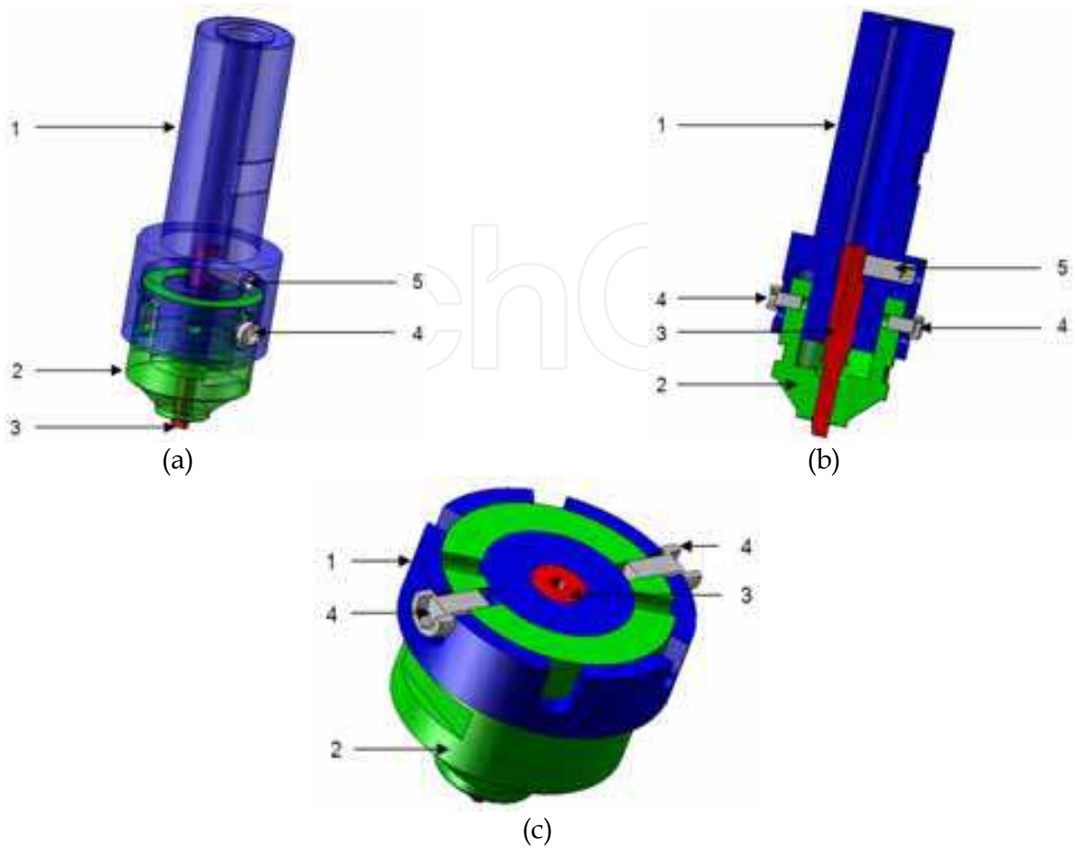

Fig. 4. Modular dual FSW tool with forced cooling.
a) 3D view of assembly, b) Viewed in longitudinal section, c) Viewed in cross section showing in detail the mechanism for adjusting the length of the probe. Nomenclature: tool body (1), built-in base (2), adjustable threaded probe with 1 mm pitch (3) screws to fix the base (4), threaded bolt fastening probe (5).

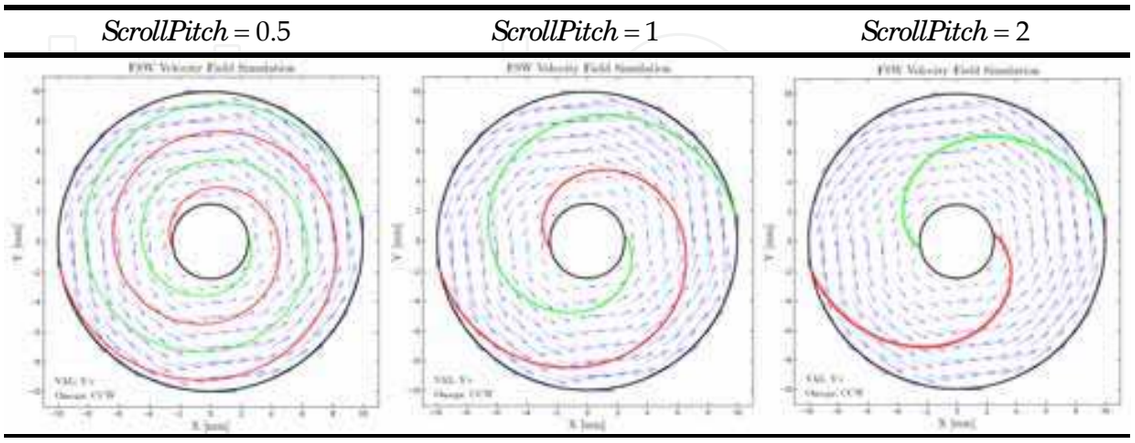

Fig. 5. Graphical representation of planar shoulders with 2 scrolls (spiral striates) for different ScrollPitch = {0.5; 1; 2}. Constant Values: Number of scrolls (striates)=2; R_{ext}=20 mm; R_{int}=5 mm; Ω=800 rpm.

2.4 Typical metallurgical features

During the FSW process, the material undergoes intense plastic deformation at elevated temperature, resulting in generation of fine and equiaxed recrystallized grains. This fine microstructure produces good mechanical properties in friction stir welds (Moreira et al., 2009). Better quality joints are associated with more intense tridimensional material flow pattern.

The typical metallurgical structures present in the processed zone of FS welds are established and classified in Figure 6. Beside the TMAZ central zone, there is the Heat affected Zone (HAZ) and the unaffected parent material or Base Material (BM)

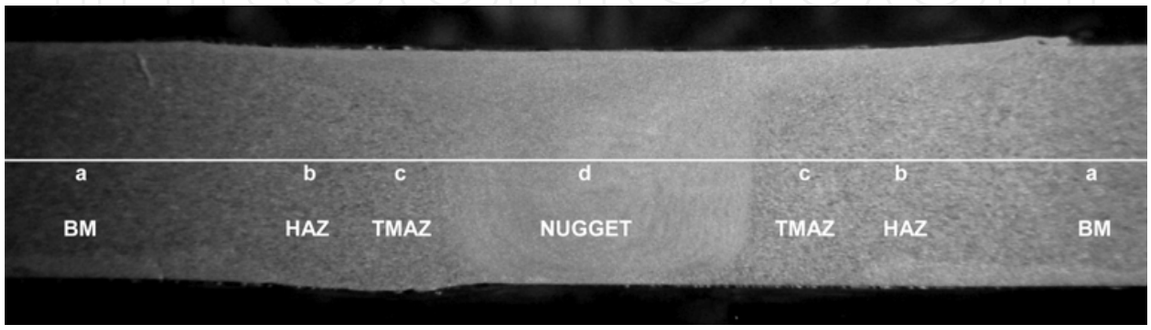

Fig. 6. Generic identification of micrograph locations

The composition of the recrystallised zone of the TMAZ (the nugget) is unchanged from that of the parent material and there is no measurable segregation of alloying elements but grain size varies across the flow contours.

Joining does not involve any use of a filler metal and therefore any lightweight metal and alloy can be joined without concern for the compatibility of the composition, which would be an issue in fusion welding. When desirable, dissimilar lightweight metal alloys and metal matrix composites can be joined with equal ease.

The principal advantages of FSW, being a solid phase process, are low distortion, absence of melt-related imperfections and high joint strength, even in those alloys that are considered non-weldable by conventional fusion techniques.

Furthermore, FSW joints are characterised by the absence of filler induced problems/imperfections. In addition, the hydrogen contents of FSW joints tend to be low, which is important in welding alloys susceptible to hydrogen damage.

3. Production and characterization of FSW samples with and without defects

3.1 Base material, FSW tools and equipment

The materials under study were AA2024-T4 and AA5083-H111 alloys, with 3.8 and 7.0 mm thickness respectively, having the chemical composition presented in Table 1. In Figure 7 it is shown the macrographs of AA2024-T4 in three different views: perpendicular and parallel to the rolling direction, and at surface of the plates.

A conventional milling machine (Figure 8a) and an ESAB LEGIO™ FSW 3UL (Figure 8b) were used to produce FSW in AA5083-H111 and in AA2024-T4, respectively. Several FSW tools geometry was tested to produce different welded conditions with and without defects. Table 3 describes the characteristics of three different FSW shoulders, and Table 4 describes the eight FSW tools tested. These tools are illustrated in Figure 9.

Material	Al	Cr	Cu	Fe	Mg	Mn	Si	Ti	Zn
AA5083-H111	94.5	0.08	0.03	0.33	4.39	0.51	0.12	0.02	0.01
AA2024-T4	93.5	max. 0.1	3.8 – 4.9	max. 0.5	1.2 – 1.8	0.3 – 0.9	max. 0.5	max. 0.15	max. 0.25

Table 2. Chemical composition of base materials as % of weight

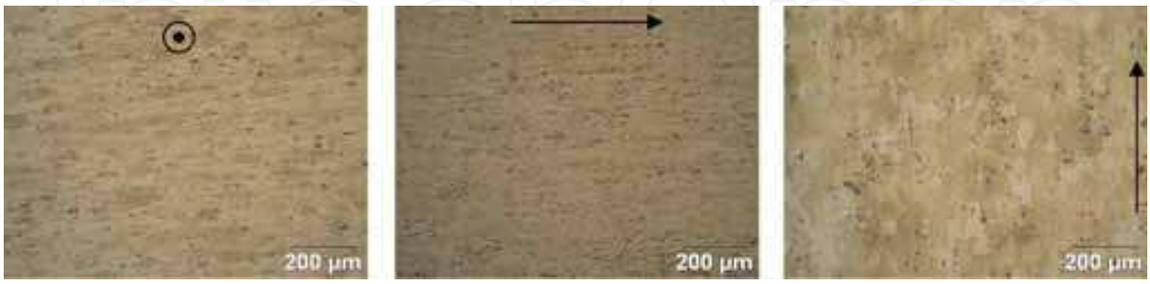

(a) (b) (c)

Fig. 7. Macrographs of AA2024-T4 perpendicular (a) and parallel (b) to the rolling direction, and in surface of the plates (c).

(a) (b)

Fig. 8. FSW equipments used to produce FSW samples. a) Conventional milling machine and the ESAB LEGIO™ FSW 3UL.

Base	$Ø_{exterior}$ [mm]	$Ø_{interior}$ [mm]	Tipo
A	15	5	Non-scrolled concave
B	19	8	Planar with spiral scrolls.and p = 2
C	18	6	Planar with spiral scrolls.and p = 0.5

Table 3. Characteristics of the FSW shoulders

Tool	Base	Probe
# 1	A	cylindrical M5 with 3 flat sided
# 2	B	conical threaded M8 with 3 helicoidal longitudinal channels (Øbase = 8 mm, Øtop = 5 mm)
# 3	B	stepped smooth surface (Øbase = 8 mm, Øtop = 6 mm)
# 4	B	conical smooth surface (Øbase = 8 mm, Øtop = 5 mm)
# 5	B	cylindrical smooth surface, with 4 helicoidally groves at the tip (Øbase = 8 mm, Øtop = 6 mm)
# 6	A	inverted conical smooth surface (Ø middle = 4 mm, Øtop = 5 mm)
# 7	A	conical smooth surface, with 1 helicoidally groves at the tip (Øbase = 8 mm, Øtop = 4 mm)
# 8	C	conical threaded with 3 flat sided (Øbase = 6 mm, Øtop = 5 mm)

Table 4. Characteristics of the FSW tools (shoulders + probes)

Fig. 9. FSW tools used to produce defect and non defect condition on AA2024-T4 and AA5083-H111

3.2 Production and characterization of FSW samples

To test and validate the NDT developed systems, some friction stir welds were produced using the above mentioned aluminium alloys AA2024-T4 and AA5083-H111.

FSW with high defects conditions were initially produced on AA5083-H111, as it shows by transverse macrograph in Figure 10. The non defect condition (Figure 10 a) correspond to a bead on plate weld, and was produced using the FSW tool #1. The high void defect condition (Figure 10 b) also corresponds to a bead on plate weld produced with the FSW

tool #1. The high void and root defect condition (Figure 10 c) was produced using the FSW tool #6. The propose of this welded conditions was to evaluate the applicability of different existent NDT techniques on FSW. This issue will be addressed in section § 4. In addition, this welded conditions was used to calibrate the Quantitative Non Destructive Testing System for FSW (QNDT_FSW) described in § 5.1, in order to compare and classify others FSW with these standard defect conditions.

(a) (b) (c)

Fig. 10. FSW produced on AA5083-H111. a) Non defect condition (bead on plate), b) High void defect condition, c) High void and root defect condition

The AA2024-T4 alloy was used to produce three different root defect conditions: Type 0, Type I and Type II (Figure 11). Defect Type 0 is characterized by some residual particles alignment in an intermittent path along ~ 150 µm. This condition is considered a non defective weld. Defect Type I is characterized by a weak or intermittent welding since the materials are in close contact, under severe plastic deformation, but with no chemical or mechanical bond along ~ 50 µm. Defect Type II is characterized by ~ 200 µm non welded zone, followed by particles alignment in an intermittent path. The three different conditions present a consecutive increase of the defect intensity, suitable for a reliability analysis of a NDT system.

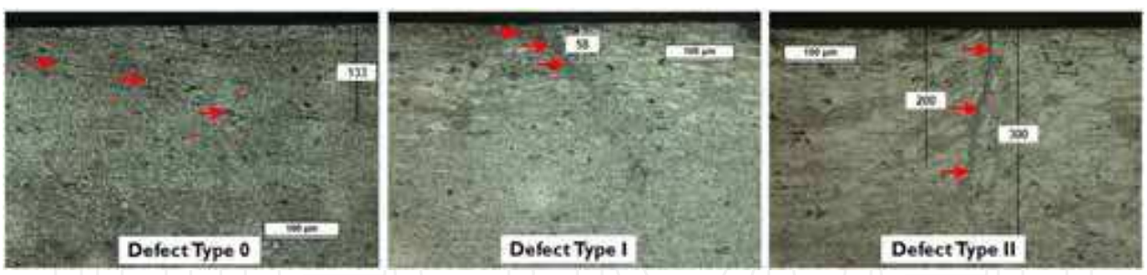

Fig. 11. Transversal macrographs of three different FSW root defects conditions on AA2024-T4 using tool # 2. Defect Type 0: particles alignment, Defect Type I: ≈ 60 µm, Defect Type II: ≈ 200 µm

Other different defects morphology was produced in AA2024-T4 alloy, exploring other FSW tools, in order to correlate the tools geometry and the weld quality of the joints. Figure 12 presents four transversal macrographs of different weld defects conditions produced with different FSW tools. Defect Type III (Figure 12 a) is an internal imperfection type void. Figures 12 a), b) and c) presents a mixed defect weld condition consisting of a root and void defects. These analyses allow concluding that the geometry of the FSW tool #2 produces the best quality welded joints.

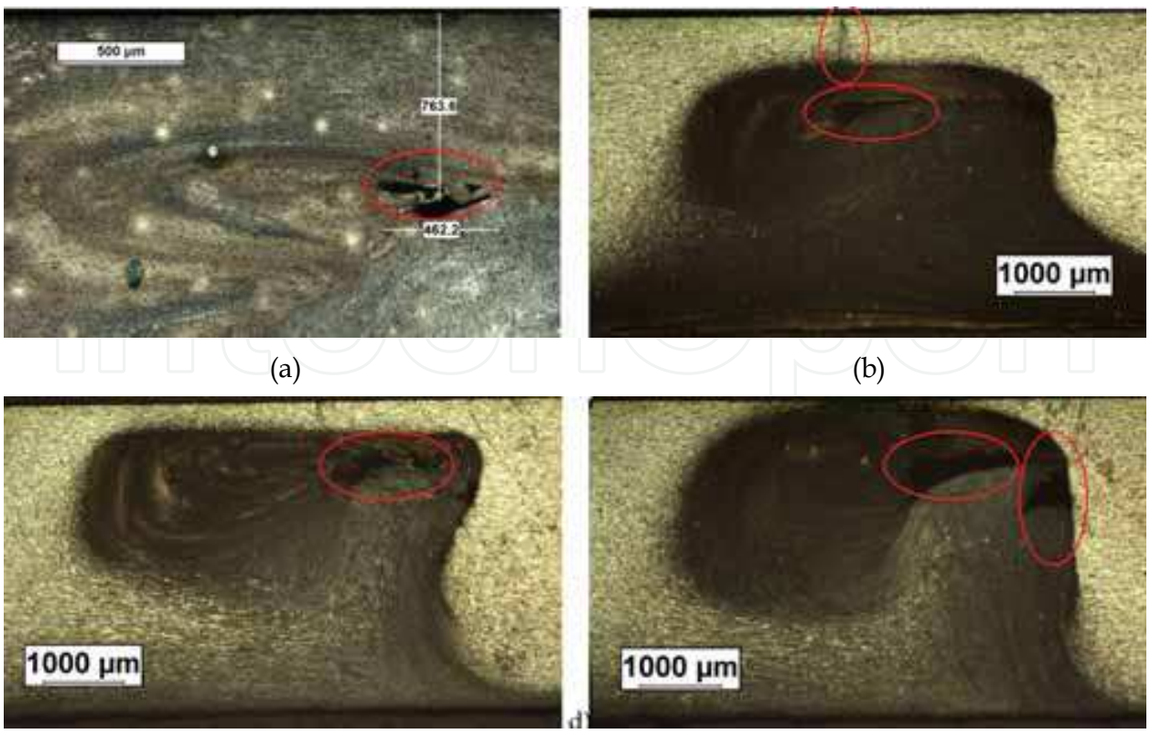

Fig. 12. Macrographs of four different FSW void and root defects conditions on AA2024-T4 a) FSW with defect Type III using tool # 2), b) FSW with defect Type M using tool # 4), c) FSW with defect Type M using tool # 6), d) FSW with defect Type M using tool # 7).

3.3 Effects of defects

Fatigue tests were performed on AA2024-T4 in order to evaluate the effects of defects on mechanical behavior of the welded joints. The propose was to identify witch defect condition (Type 0, Type I, Type II and Type III) presents a significantly decrease of fatigue life comparing to the base material.

The fatigue tests are performed on an Instron 8874, with a load cell of 25kN. Stress ratio R is 0.1. The S-N curve results obtained are presented in Figure 13 (Santos et al., 2009). This result leads to conclude about the good mechanical efficiency of the FSW joints with Defect Type 0. In fact, these joints present a mechanical behaviour similar to the base material. Concerning to the other three defect types, all presents a significantly loss of mechanical resistance. Among these different defects, the root defects (Type II) are definitely the ones that show higher loss of mechanical properties under fatigue loading. Those imperfections are thereby the NDT targets defects of FSW. Furthermore, the other type of imperfections (e.g. thickness reduction and flash formation) may be inherent to the process itself and are impossible to be avoided or may be evaluated without need of NDT.

4. Evaluation of the applicability of conventional NDT techniques to FSW

In order to evaluate the applicability of conventional NDT techniques to FSW some experimental tests were performed on above described defects conditions on AA2024 – T4

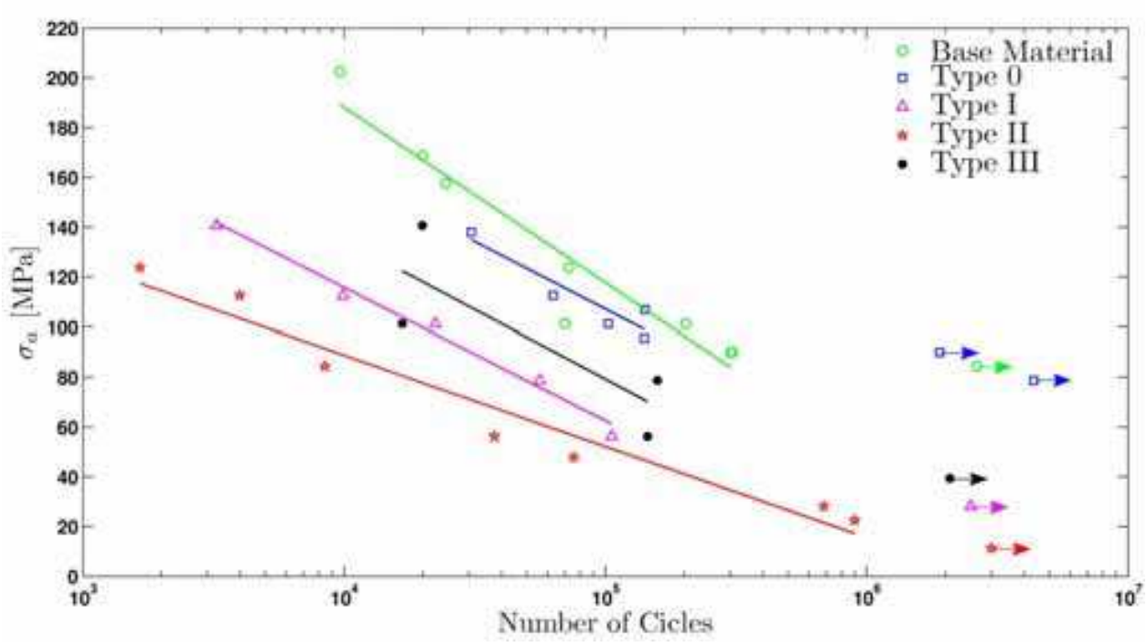

Fig. 13. Fatigue curves for base material and 4 different defect type conditions

and AA5083-H111. The propose is to conclude about the capability of conventional NDT techniques to detect the FSW defects with the morphologies described in section § 3.2.

4.1 Conventional X-ray

The specimens were analyzed using conventional X-Rays, in Scan-Ray® equipment, DOA 300/AC-103 model, rightly calibrated and certificated. AGFA® D4 X-Ray film, an extra fine grain film with very high contrast, and with density value of 2 was used for these trials.
The X-ray parameters were: Intensity: 5mA; Energy: 70 kV; Exposure time: 150 sec; Distance between the source and the film: 800 mm.
The friction stir welds were oriented with the root to the X-ray film in order to avoid image distortion in the cases that the defect at the root was detected. The quality image control and the acquirement of the sensitivity values were done with a pattern behind the sample, in accordance of the standard DIN 54109 and recommended by the International Institute of Welding.
In Figure 14 it is present the X-ray image of specimens produced on AA5083-H111 with high defects type voids and roots similar to the ones presented in Figure 10 a and Figure 10 b). It is possible to observe that booth root and internal defects are visible, since they are very big. However, X-ray NDT technique cannot detect FSW micro root defects whit the morphology described in Figure 11. In Figure 15 and Figure 16 it is presented X-ray image of specimens produced on AA2024-T44 with root defect Type II and void defect Type III, respectively. The acquired image (Figure 15) show that even the biggest root defect (Type II) was not detected. Only defect Type III (void defect) was detected, as it shows in Figure 15.

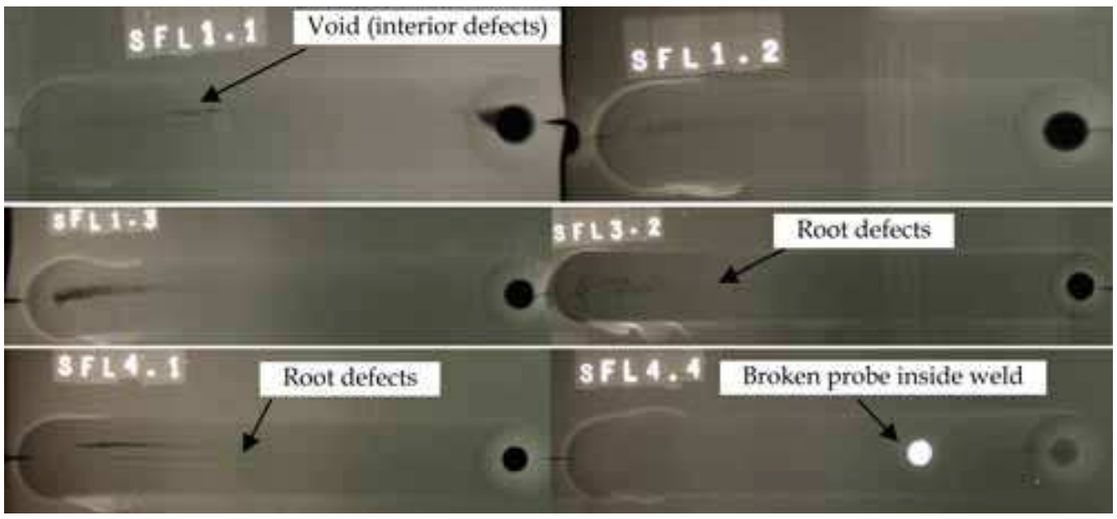

Fig. 14. X-ray image of specimens produced on AA5083-H111 with high voids and roots defects

Fig. 15. X-ray image of specimens produced on AA2024-T4 with roots defects Type II

Fig. 16. X-ray image of specimens produced on AA2024-T4 with void defects Type III

4.2 Conventional creping ultra-sound

Creeping ultrasonic inspection was performed with a 4 MHz probe, on both retreating and advancing sides of the weld, where the insonification direction was always perpendicular to the welding direction (Figure 17). Gathering data from both sides of the weld created a redundancy of data, which was analyzed by the data fusion algorithm of the QNDT_FSW described in § 5.1. Creeping inspection was also complemented with data that came from

attenuation measurements. The measurement of the attenuation is performed with an ultrasonic probe working in receiving mode, located at the opposite side of the weld bead in the same insonification plane of the creeping probe. Therefore, in the case of defect, a creeping signal change occurs, increasing at the same time the attenuation. These two simultaneous conditions allowed the QNDT_FSW system to distinguish between signal disturbance and real imperfections.
The results of the NDT creeping ultra-sound on AA5083-H111 presented in Figure 18 show that the high root defects was detected by a signal change, underline by the red boxes. However, once again, the micro root defects presented in AA2024-T4 was not detected.

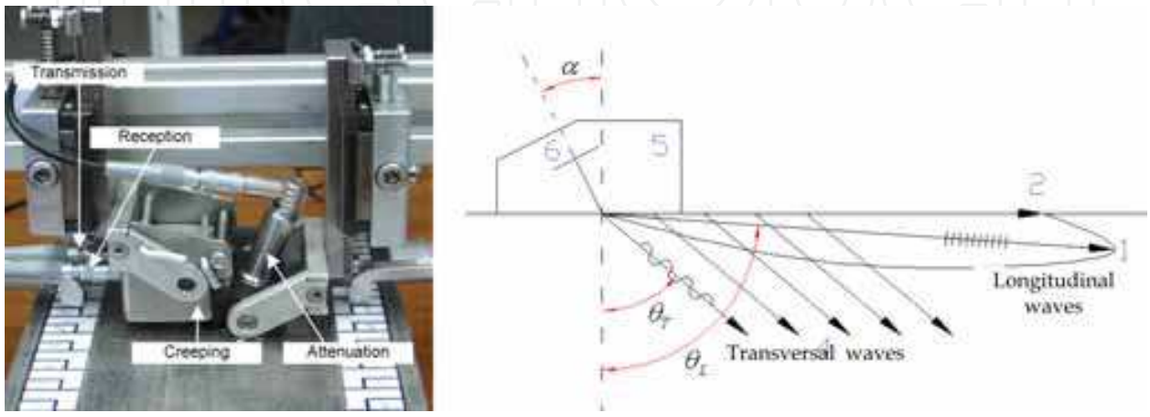

a) b)

Fig. 17. Inspection of FSW with conventional creping ultra-sound.
a) Creeping and attenuation probes displacement, b) Schematic representation of the ultra-sound waves in the material AA6083-H111.

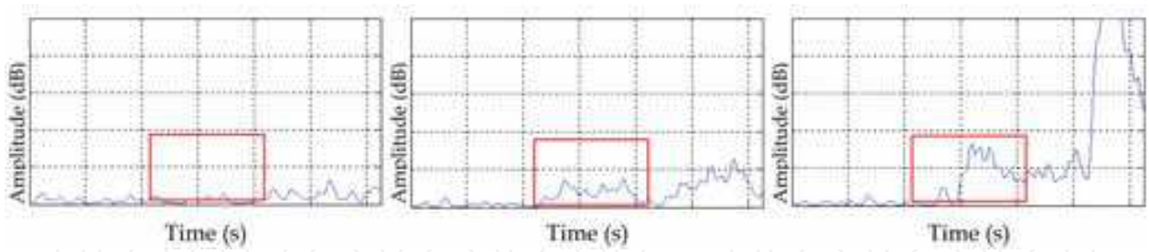

a) b) c)

Fig. 18. Results of the NDT creeping ultra-sound on AA5083-H111.
a) Non defect condition (bead on plate) of Figure 10 a, b) Moderate FSW root defect condition, c) High void and root defect condition of Figure 10 c.

4.3 Time of Flight Diffraction (ToFD)

Time of Flight Diffraction (ToFD) NDT technique was performed with a 15 MHz probes on the same samples described in above section § 4.2. Figure 19 shows the used arrangement of the probes and the motion device. Once again, the results presented in Figure 20 shown that ToFD technique was able to identify high root and void defects in AA5083-H11 samples, by a evident signal change underline by the red boxes. Nevertheless, the micro root defects presented in AA2024-T4 was not detected.

a) b)

Fig. 19. ToFD ultra-sound NDT testing of AA5083-H111.
a) 15 MHz ToFd probes used, b) Arrangement of the probes and motion device.

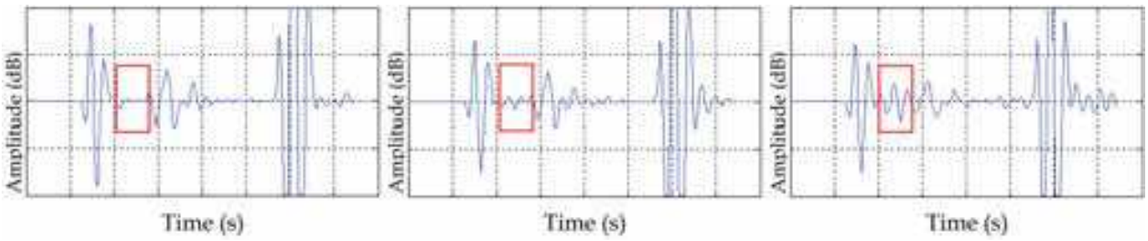

a) b) c)

Fig. 20. Results of the NDT ToFD ultra-sound on AA5083-H111.
a) Non defect condition (bead on plate) of Figure 10 a, b) Moderate FSW root defect condition, c) High void and root defect condition of Figure 10 c.

4.3 Conventional Eddy Current (EC)

The three FSW defect conditions Type 0, Type I and Type II in AA2024-T4, described in Figure 11 (section § 3.2) were inspected by NDT eddy current (EC) technique using a conventional cylindrical helicoidally EC probe.

The signal was acquired from the root side, along a sweep on the transversal direction to the weld joint. The starting point of the tests was set to 25 mm in the retreating side of the weld bead, and 50 mm long segments were characterized in direction to the advancing side, with 250 µm space within each acquisition. In all the acquisitions the real and imaginary part of electrical impedance was measured @ f = 400 kHz.

In Figure 21 it is presented the obtained results S(x) = Abs{Z}. It can be seen that the three curves concerning to the previously defects conditions present a very similar trend between them.

It means that the conventional probes have very low sensitivity to root defects. The reason is that the impedance changes are mainly due to the presence of the FSW weld bead, instead the presence of a defect. In fact the FSW process causes microstructural modifications (Nascimento et al., 2009) material conductivity changes in the bead zone, even without any imperfections. Therefore there is no distinctive signal feature that can allow to distinct between each defect condition. Indeed, the absolute conventional probe can only reproduce the global spreaded increase of conductivity field due to the FSW bead. Such probes are not

able to distinguish small suddenly variations of conductivity, caused by a local micro root defect as those tested (Santos et al., 2009). These results illustrate the difficulty of NDT of FSW when using conventional EC probes.

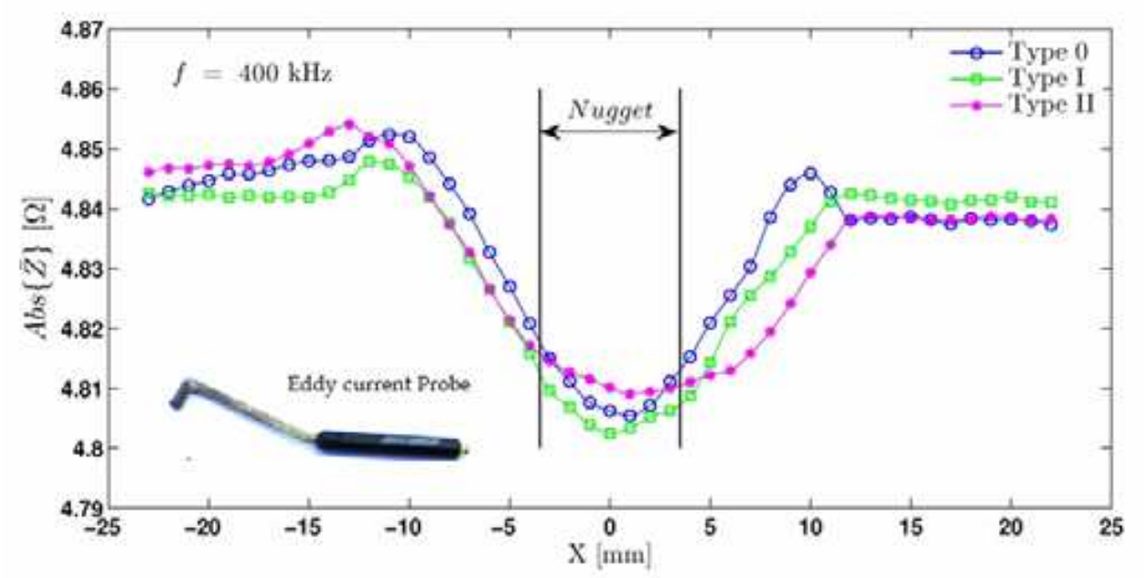

Fig. 21. Results for the NDT inspection of FSW joints with defect Types 0, I and II @ f = 400 kHz using a conventional cylindrical helicoidally EC probe.

5. Recent advances in NDT for FSW of aluminium alloys

5.1 QNDT_FSW: Inspection system for FS welds based on data fusion

The Quantitative Non Destructive Testing for FSW (QNDT_FSW) is an integrated, on-line system. It employs a data fusion algorithm to improve the confidence of inspection based on Relative Operating Characteristics (ROC) and Probability of Detection (PoD). The complementary and redundant data acquired from several NDT techniques generate a synergistic effect, which is the main advantage of the present approach. The data fusion algorithm uses fuzzy logic and fuzzy interference functions to mingle the data from several NDT techniques.

The QNDT_FSW system incorporates three, distinct NDT techniques. They include a 4 MHz creeping ultrasonic probe, a 15 MHz Time of Flight Diffraction (ToFD) probe, a 20 kHz eddy current probe, and a 2 MHz eddy current probe. These techniques were selected to detect, as much as possible, the position and diversity of imperfections in FS welds (Santos et al., 2008).

Among the several FSW trials performed to validate and implement the QNDT_FSW system, one application samples are presented. The results of testing the QNDT_FSW system are presented in terms of equivalent imperfection indices called the Root Imperfection Index (RII) and the Internal Imperfection Index (III). These imperfection indices were calculated with fusion inference functions and represent the data fusion result for all of the above mentioned NDT techniques. Figure 22 illustrates algorithm to calculate IRD and III.

An imperfection index equal to 100 % means a high-imperfection weld section, similar to the high-imperfection weld standard of the Figure 10 b and c). An imperfection index equal to 0 % means an imperfection-free weld section, similar to imperfection-free weld standards of the Figure 10 a).

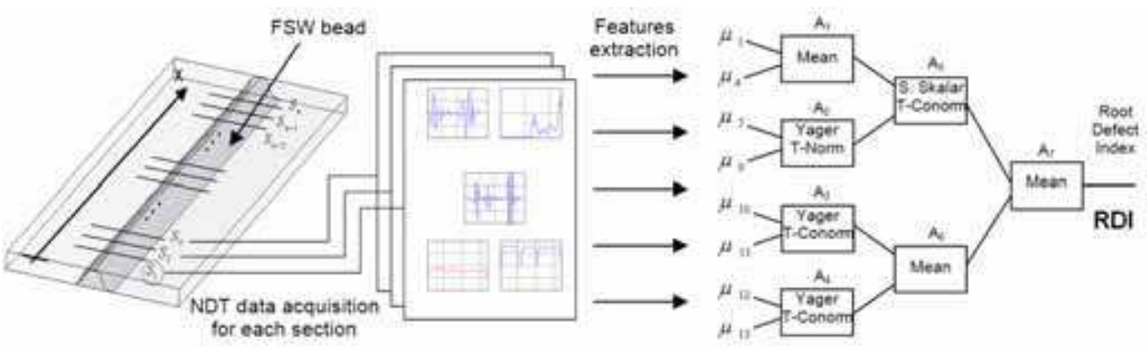

Fig. 22. Schematic representation of the algorithm to calculate IRD and III

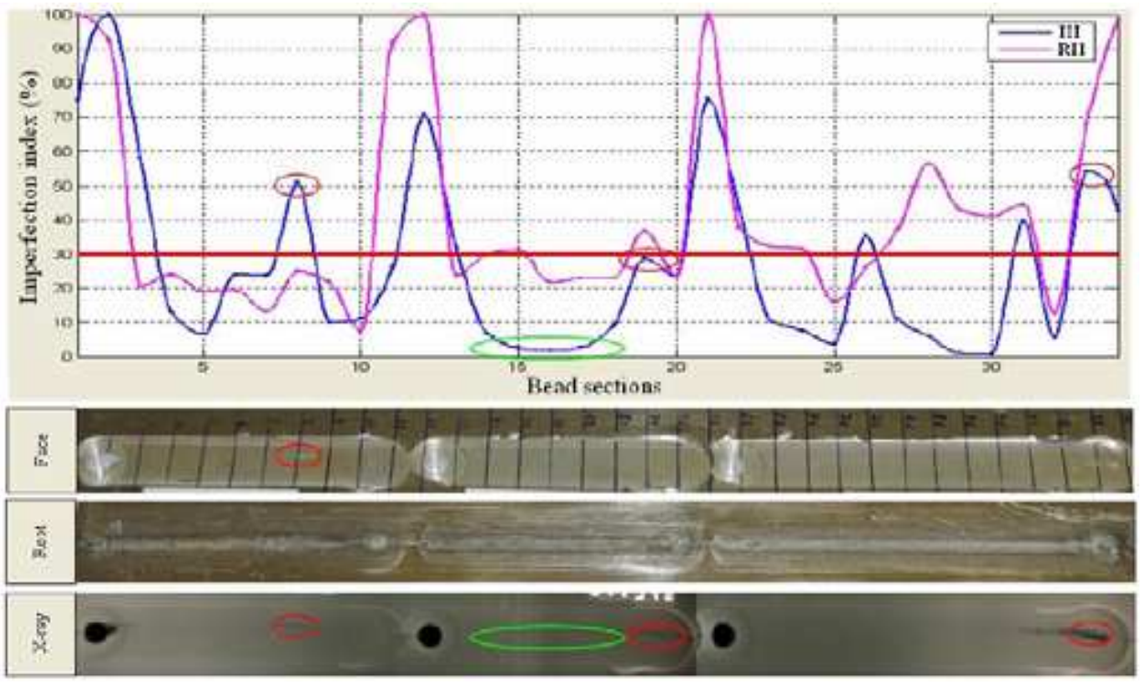

Fig. 23. RII and III for three consecutive welds on AA5083-H111

Figure 22 presents the results of applying the QNDT_FSW system to three different FSW trials on AA5083-H111. The trials were performed with a probe length of 6.8 mm, a tilt angle of 2º, and a rotation speed of 710 rpm. The difference between these 3 trials was a change in the travel speed. In section 11 to section 1, the travel speed was 160 mm/min; from section

21 to section 12, the travel speed was 224 mm/min; and from section 34 to section 22, the travel speed was 320 mm/min. Based on a comparison (Figure 23) of the RII and III results with the macroscopic, visual, and radiographic test results, the following conclusions were made:

- The exit holes located at sections 1, 12 and 22 were detected by both imperfection indices;
- In section 8, the III revealed a cavity, which was corroborated by radiographic testing and visual inspection as the cavity breaks the surface of the workpiece. Moreover, the RII was not affected, which confirmed the independence of both imperfection indices;
- Sections 14 to 18 present a very low III, which was corroborated by radiographic testing. RII was able to detect small, root imperfections, as confirmed by metallographic cross-sections of the weld. Emphasis should be given to the fact that in these sections, radiographic testing cannot detect a root imperfection;
- For the 3 FSW trials, the RII increased as the travel speed increased. This behaviour was expected because the probe length was 0.2 mm shorter than the plate thickness. This created a small root imperfection that increased with increased in size as the travel speed increased.

The proposed equivalent defect indices for evaluating the significance of root (RII) and internal (III) imperfections show that the results accurately predicted the quality of the weld. In fact, combining the data from several NDT processes is an improvement, when compared to interpreting the individual results of each NDT process, due to the synergistic effect of the data fusion algorithm.

5.2 Eddy current IOnic probe

In order to improve the reliability in FSW non-destructive inspection a new NDT EC system with a special designed probe was developed and tested in AA2024-T4 FSW defects conditions. The EC probe allows a 3D induced eddy currents in the material; deeper penetration; independence of the deviation between the probe and the material surface; and easy interpretation of the output signal based on a comprehensible qualitative change.

The so called IOnic (Rosado et al., 2010) probe is constituted by one excitation filament, in the middle of two sensitive planar coils, in a symmetric configuration (Figure 24). Due to this layout the operation of the IOnic probe is based on an integration effect along each sensitive coil, and simultaneous, on a differential effect between the two coils. The probe was manufactured on 1.6 mm dual layer FR4 PCB subtract with an external diameter of 11 mm. The two sensitive coils are formed by tracks of 100 µm width separated by same dimension gaps.

The IOnic probe has some other advantages when compared to the conventional eddy currents probes: i) precision differential based operation resulting on high sensibility and superior lift-off immunity; ii) improved contact with test material by being planar, leading to deeper eddy currents penetration in test material; iii) the straight eddy currents induced in the material near the driver trace can be taken as advantage to evaluate materials where the flaws tend to follow a specific orientation; iv) allow the inspection of the material borders as long as the symmetry axis remains perpendicular to it; v) can be implemented in flexible substrates easily adaptable to non-planar and complex geometry surfaces.

The eddy current NDT System for FSW includes further dedicated components, namely: i) electronic devices for signal generation, conditioning and conversion, ii) automated mechanized scanning, and iv) dedicated software, shown in Figure 25.
The IOnic Probe was applied on AA2024-T4 defects condition Type 0, Type I and Type III described before in Figure 10. The data $S(x) = \mathrm{Im}\{\bar{U}out/\bar{I}\}$ was acquired from the root side, along a sweep on the transversal direction to the weld joint, with the excitation filament of the probe parallel to weld joint. The inspection was perform @ f = 50 kHz, f = 100 kHz and f = 250 kHz. The imaginary part of the three types of defects at these frequencies is shown in Figure 26.

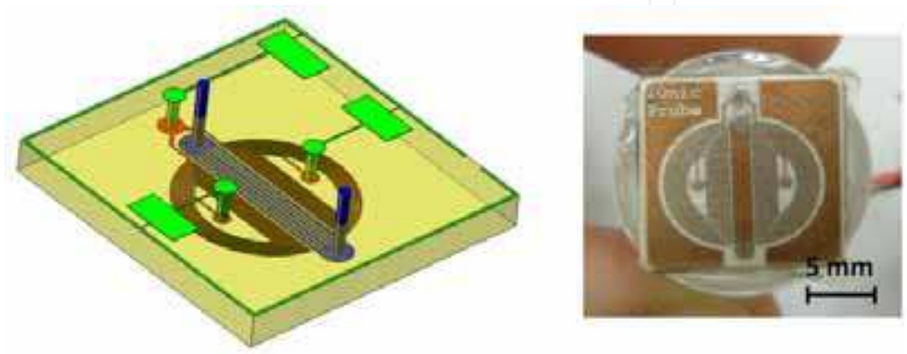

Fig. 24. The IOnic Probe prototype.

Fig. 25. NDT system overview: laboratory apparatus for inspecting FS welds: the mechanical support system device and the computational data acquisition device.

As FSW process causes material conductivity changes, even without imperfections, the weld bead is responsible for the large curve on the imaginary part. The presence of imperfections creates a small perturbation observed on the middle of the joint, highlighted in red. This small perturbation observed at the middle of the joint concerns to the suddenly decrease of conductivity due to the local root defect of each defect condition. Notice that there is a very good proportionality between the defect dimension and the observed perturbation on the imaginary part Im{Ūout/Ī}. These results show that IOnic probe is able to identify the three different types of defect conditions produced in AA2024-T4 aluminum alloy.

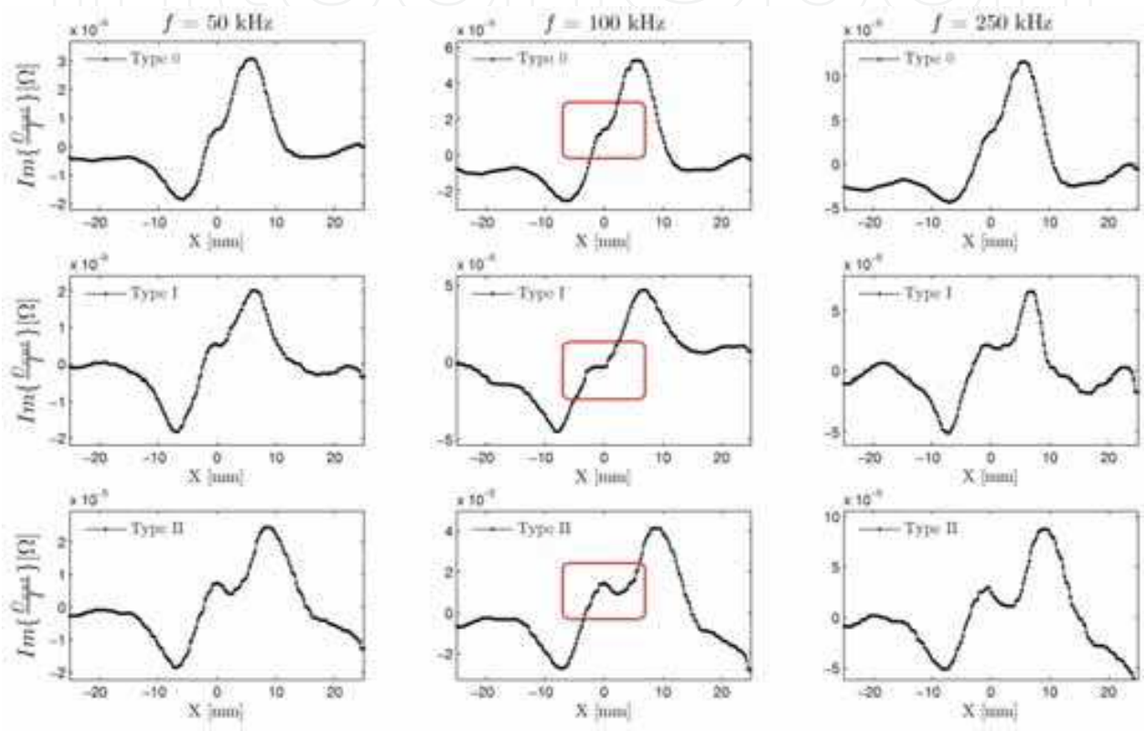

Fig. 26. Results of IOnic Probe for the FSW joints with defect types 0, I and II @ f = 50 kHz, f = 100 kHz and f = 250 kHz.

6. Conclusion

From the present work the following conclusions can be drawn:
Micro root defects in friction stir welds as the lack of penetration or kissing bond are defects endorsed by failures in the process parameters that can occur in industrial applications. These defects weaken the structural fatigue strength that in critical structural are not tolerated. In this way, effective and reliable nondestructive techniques are required for the detection of these flaws.
The geometry, location and microstructural nature of the FSW defects, which bore no resemblance with defects typical of fusion welding of aluminium alloys, lead to very difficulties in identification when using the common NDT techniques.

Conventional NDT techniques such as creeping ultrasound, ToFD, X-ray or axis-symmetry eddy current probes are not able to detect the typical FSW micro root defects with depth below 200 μm.

A NDT integrated data fusion system for FSW named QNDT_FSW was presented. Equivalent defective indexes are proposed for evaluating the relevance of the root (RDI) and internal (IDI) defects. The data fusion algorithm for NDT of FSW, based on fuzzy logic and fuzzy inference functions disclosed a general powerful data fusion NDT approach. Combining the data from several NDT processes is an improvement, when compared to interpreting the individual results of each NDT process, due to the synergistic effect of the data fusion algorithm.

The experiments shown that the IOnic Probe is able to identify different levels of FSW micro root defects by a qualitative perturbation of the output signal. It was also shown that exist a good proportionality between the defects size and this signal perturbation.

7. Acknowledgements

The authors would like to acknowledge Fundação para Ciência e Tecnologia (FCT) for its financial support via project POCTI/EME/60990/2004

8. References

Moreira, P. M. G. P., T. Santos, S. M. O. Tavares, V. Richter – Trummer, P. Vilaça, P. M. S. T. de Castro, (2009), Mechanical and metallurgical characterization of friction stir welding joints of AA6061 – T6 with AA6082 – T6, Materials and Design (ISSN: 0261-3069); Vol. 30, Issue 1, pp.180 – 187;

Nascimento, F., T. Santos, P. Vilaça, R.M. Miranda, L. Quintino, (2009), Microstructural modification and ductility enhancement of surfaces modified by FSP in aluminium alloys. International Journal of Materials Science and Engineering: A (Structural Materials: Properties, Microstructure and Processing). Vol. 506, N.º 1 – 2, pp. 16 – 22,. DOI:10.1016/j.msea.2009.01.008.

Rosado, Luís, Telmo G. Santos, Moisés Piedade, Pedro Ramos, Pedro Vilaça, (2010) Advanced technique for non-destructive testing of friction stir welding of metals, Measurement (ISSN: 0263-2241); doi:10.1016/j.physletb.2003.10.071

Santos, T., P. Vilaça, L. Quintino, (2008), Developments in NDT for Detecting Imperfections in Friction Stir Welds in Aluminium Alloys. Welding in the World (ISSN 0043 – 2288), Journal of the International Institute of Welding (IIW), Vol. 52, N.º 9 – 10, pp.30 – 37;

Santos, Telmo, Pedro Vilaça, Luísa Quintino, (2009), Computational Tools For Modeling FSW and An Improved Tool for NDT, Welding in the World (ISSN: 0043 – 2288), Journal of the International Institute of Welding (IIW), (IIW-1978-08 (ex-doc. III-1507r1-08), Vol. 53, N.º 5/6;

Thomas W M, Nicholas E D, Needham J C, Murch M G, Temple-Smith P, and Dawes C J (1991) Improvements relating to friction stir welding. US Patent No. 5,460,317.

Thomas Wayne M. (2009). PhD thesis: *An Investigation and Study into Friction stir Welding of Ferrous-Based Material*, University of Bolton.

Vilaça, P, (2003). PhD thesis: Fundamentos do Processo de Soldadura por Fricção Linear - Análise Experimental e Modelação Analítica, Instituto Superior Técnico, Technical University of Lisbon.

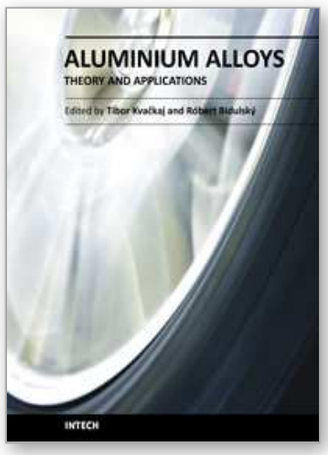

Aluminium Alloys, Theory and Applications

Edited by Prof. Tibor Kvackaj

ISBN 978-953-307-244-9
Hard cover, 400 pages
Publisher InTech
Published online 04, February, 2011
Published in print edition February, 2011

The present book enhances in detail the scope and objective of various developmental activities of the aluminium alloys. A lot of research on aluminium alloys has been performed. Currently, the research efforts are connected to the relatively new methods and processes. We hope that people new to the aluminium alloys investigation will find this book to be of assistance for the industry and university fields enabling them to keep up-to-date with the latest developments in aluminium alloys research.

How to reference

In order to correctly reference this scholarly work, feel free to copy and paste the following:

Pedro Vilaça and Telmo G. Santos (2011). Non-Destructive Testing Techniques for Detecting Imperfections in Friction Stir Welds of Aluminium Alloys, Aluminium Alloys, Theory and Applications, Prof. Tibor Kvackaj (Ed.), ISBN: 978-953-307-244-9, InTech, Available from: http://www.intechopen.com/books/aluminium-alloys-theory-and-applications/non-destructive-testing-techniques-for-detecting-imperfections-in-friction-stir-welds-of-aluminium-a

INTECH
open science | open minds

InTech Europe
University Campus STeP Ri
Slavka Krautzeka 83/A
51000 Rijeka, Croatia
Phone: +385 (51) 770 447
Fax: +385 (51) 686 166
www.intechopen.com

InTech China
Unit 405, Office Block, Hotel Equatorial Shanghai
No.65, Yan An Road (West), Shanghai, 200040, China
中国上海市延安西路65号上海国际贵都大饭店办公楼405单元
Phone: +86-21-62489820
Fax: +86-21-62489821

IntechOpen